THE ASTROPHYSICAL JOURNAL SUPPLEMENT SERIES, 47:229–233, 1981 November

A NEAR-INFRARED ATLAS OF SPIRAL GALAXIES

DEBRA MELOY ELMEGREEN
The Mount Wilson and Las Campanas Observatories, Carnegie Institution of Washington[1]
Received 1981 February 11; accepted 1981 April 17

ABSTRACT

A near-infrared photographic atlas of 54 spiral galaxies is presented. Blue photographs are included so that features may be compared in the two passbands. Hubble types range from Sa through Sd for SA, SAB, and SB galaxies. Most are nearly face-on and larger than 2′. These galaxies have been subdivided into the subjective categories of grand design and flocculent spirals, depending upon the appearance of their spiral arms. Photographic procedures and their effects are discussed.

Subject headings: galaxies: stellar content — galaxies: structure — infrared: general

I. INTRODUCTION

Morphological studies of galaxies began with the discovery of the spiral shape of M51 by Lord Rosse in 1845. Most photographic surveys, such as the Hubble Atlas (Sandage 1961), have been made in the *B* or *V* passbands. These wavelengths are suitable for examining the young stars and dust obscuration, which provide information about the locations of star formation and of large-scale gas compressions in a galaxy. The distribution of older stars is more evident at longer wavelengths. Schweizer (1976) showed that the contribution of OB stars to the total intensity is only 15% in the near-infrared, compared with 65% in the blue; most of the light in the smooth underlying red arms is emitted by older disk main sequence and giant stars. The stellar morphology is also prominent in the *I* band because the opacity of dust is 2.6 times less than in the *B* (Johnson 1966).

This paper introduces a near-infrared photographic atlas of spiral galaxies with Hubble types Sa through Sd. The primary classification of spiral galaxies is based upon the size of the bulge or nuclear region and the tightness of the winding of the spiral arms (see review by Sandage 1975). In addition to this formal classification, subdivisions may be made according to the structure of the spiral arms. Although a continuum of arm subdivisions may exist, it is useful to mention the two extreme cases. The first comprises the M51-type galaxies, which are said to have a "global" or "grand design" spiral pattern. In these galaxies, the arms are long and continuous, and there is a two-armed axial symmetry. The second group consists of galaxies in which the spiral arms are highly fragmented in visual photographs. These galaxies have arms whose continuity extends only over small angles; the spiral pattern is composed of many patchy arm segments. Sandage (1961) first alluded to these galaxies by mentioning several early-type galaxies that are similar to the prototype, NGC 2841. Woltjer (1965) distinguished such galaxies from the grand design spirals by referring to them as "spiral-like". Kormendy (1977) also emphasized their distinctiveness as a group. These NGC 2841–type or spiral-like galaxies will be referred to as "flocculent" spirals to underscore their patchy appearance, a characteristic that is independent of Hubble type.

The contrasting appearance of grand design and flocculent spiral galaxies suggests that their predominant morphologies may be a result of different spiral structure formation mechanisms (e.g., compare Lin and Shu 1964 or Roberts, Roberts, and Shu 1975 with Mueller and Arnett 1976 or Gerola and Seiden 1978). There is probably some interplay between density waves and stochastic or other processes in creating spiral morphology. The possibility of the presence of more than one process was first suggested and examined theoretically by B. Elmegreen (1979), and has been inferred observationally in detail for one galaxy, M83 (Jensen, Talbot, and Dufour 1981).

The galaxies in this atlas have been subdivided into grand design and flocculent groups. At the present, these are subjective categories that are based on the appearances of the most prominent features that are present on sky-limited blue plates. Forthcoming surface photometry on the galaxies in this atlas will provide a quantitative analysis that will allow intermediate cases to be discerned more easily; for example, there may be low amplitude or narrow patterns of symmetric, continuous arms present in the galaxies classified as flocculent. The present atlas serves to illustrate the main characteristics of grand design and flocculent galaxies. One motivation for this study was to determine whether

[1]Most observations were made at Palomar Observatory as part of a collaborative agreement between CIT and CIW.

galaxies with flocculent spiral structure in visual wavelengths appear to be smoother and more regular in the near-infrared, as are the grand design spirals. It is shown here that blue-flocculent galaxies are also patchy in the near-infrared.

II. OBSERVATIONS

a) Galaxies in the Near-Infrared Atlas

Fifty-four galaxies with Hubble types Sa through Sd are presented in this atlas. They were selected to have a small inclination to the line of sight, which allows a favorable view of the morphology, and a large angular size, which provides finer resolution of the spiral structure. Most galaxies have inclinations less than 55° and maximum dimensions in excess of 2′.

Each of the galaxies in this atlas were classified according to whether they exhibit more of the characteristics of a grand design galaxy or of a flocculent galaxy. This simplistic division was made in order to emphasize the dominant features of the two types. Criteria for classification as a grand design galaxy included the presence of smooth, continuous long arms and a two-armed symmetry. The appearance of short, broken-up arms defined the flocculent members. This subjective classification is suitable because all of the plates have similar exposure times and resolutions. The more notable intermediate cases in this atlas include NGC 925, 1784, 2715, 2903, 3486, 3675, 5033, and 6643.

The 37 grand design galaxies in this atlas are listed in Table 1 and are shown in Figures 1 through 13 (Plates 1-13); the 17 flocculent spiral galaxies are listed in Table 2 and displayed in Figures 14 through 19 (Plates 14-19). Column (2) of each table lists the classifications of the galaxies (de Vaucouleurs, de Vaucouleurs, and Corwin 1976), and column (3) gives the scale of the photographs

TABLE 1

CATALOG OF GRAND DESIGN SPIRAL GALAXIES

Name	Classification	Print Size (arc min per vertical length of photo)
NGC 3031 (=M81)	SA(s)ab	23.2
NGC 5194 (=M51)	SA(s)bcp	13.4
NGC 628 (=M74)	SA(s)c	9.7
NGC 4254 (=M99)	SA(s)c	7.5
NGC 598 (=M33)	SA(s)cd	51.1
NGC 3504	RSAB(s)ab	8.0
NGC 157.....	SAB(rs)bc	6.9
NGC 2903	SAB(rs)bc	12.5
NGC 3344	RSAB(r)bc	9.8
NGC 4321 (=M100) ...	SAB(s)bc	9.5
NGC 5248	SAB(rs)bc	7.7
NGC 6384	SAB(r)bc	5.9
NGC 6951	SAB(rs)bc	5.9
NGC 7753	SAB(rs)bc	5.7
NGC 309.....	SAB(r)c	5.8
NGC 1232	SAB(rs)c	7.5
NGC 1637	SAB(rs)c	4.8
NGC 2715	SAB(rs)c	8.0
NGC 3486	SAB(r)c	8.0
NGC 6181	SAB(rs)c	2.8
NGC 5457 (=M101) ...	SAB(rs)cd	27.5
NGC 6946	SAB(rs)cd	14.2
NGC 7424	SAB(rs)cd	12.4
IC 342	SAB(rs)cd	26.1
NGC 925.....	SAB(s)d	10.4
NGC 4314	SB(rs)a	4.6
NGC 4274	RSB(r)ab	4.6
NGC 1097	SB(s)b	11.4
NGC 5383	SB(rs)b:p	22.5
NGC 1300	SB(rs)bc	6.9
NGC 3992	SB(rs)bc	7.8
NGC 1832	SB(r)bc	5.1
NGC 1073	SB(rs)c	7.5
NGC 2835	SB(rs)c	10.9
NGC 3359	SB(rs)c	9.9
NGC 7479	SB(s)c	5.7
NGC 3319	SB(rs)cd	11.2

TABLE 2

CATALOG OF FLOCCULENT SPIRAL GALAXIES

Name	Classification	Print Size (arcmin per vertical length of photo)
NGC 7217 ...	RSA(rs)ab	5.3
NGC 488	SA(r)b	7.3
NGC 2841 ...	SA(r)b:	10.1
NGC 3675 ...	SA(s)b	8.4
NGC 5055 ...	SA(rs)bc	9.8
NGC 4298 ...	SA(rs)c	7.5
NGC 4414 ...	SA(rs)c?	5.0
NGC 5033 ...	SA(s)c	12.0
NGC 6643 ...	SA(rs)c	5.3
NGC 6015 ...	SA(s)cd	5.3
NGC 7793 ...	SA(s)dm	9.7
NGC 5005 ...	SAB(rs)bc	8.1
NGC 253	SAB(s)c	50.2
NGC 1961 ...	SAB(rs)c	6.0
NGC 2403 ...	SAB(s)cd	10.2
NGC 1784 ...	SB(r)c	6.9
NGC 2500 ...	SB(rs)d	8.9

in Figures 1 through 19, in arc minutes per vertical length of each print.

The galaxies are listed in the tables and arranged in the figures in order of increasing Hubble type, from Sa through Sd, within the three main de Vaucouleurs divisions SA, SAB, and SB. The blue and near-infrared photographs have been reproduced on the same scale and printed side by side for each galaxy in order to facilitate comparison of the morphologies in the two passbands.

b) Photographic Procedures

Fifty of the galaxies were observed with the 1.2 m Schmidt telescope at Palomar Observatory. The remaining four galaxies were observed at the Cerro Tololo Inter-American Observatory: NGC 628, 7424, and 7793 using the 4 m telescope, and NGC 253 using the 0.6/0.9 m Curtis-Schmidt telescope. The plate scales are $\sim 67''$ mm^{-1} for the Palomar Schmidt, $19''$ mm^{-1} for the CTIO 4 m, and $96''$ mm^{-1} for the CTIO Schmidt.

The near-infrared survey was made with IV-N emulsions. These plates were hypersensitized by soaking for 4^m in a 2% solution of $AgNO_3$, followed by 30^s in a one-third strength photo-flo solution. Techniques are discussed by Jenkins and Farnell (1976), Hoessel (1978), Schoening (1978), and Pinto (1979). The plates were exposed behind a Wratten 88A filter which transmits wavelengths longer than 7300 Å, so that Hα light is avoided. This plate-filter combination provides an effective wavelength of 8250 Å for a flat spectrum. Exposure times were 2^h on the Palomar Schmidt (1^h on the Curtis-Schmidt and 4 m), and the plates are sky limited. Seeing was typically $2''$ during the exposures, as estimated visually at the telescopes.

Blue plates were also taken of each galaxy to provide a comparison with the near-infrared plates. For this purpose, 103a-0 emulsions were baked for 2^h45^m in forming gas at 65° C, and exposed behind a GG385 filter for 12^m at the Palomar Schmidt (25^m on the Curtis-Schmidt and 30^m on the 4 m) to obtain sky-limited plates. The gray spectrum effective wavelength for this plate-filter combination is 4360 Å. All plates were developed for 5^m in D-19 in a rotating rocker tray.

Blue or visual photographs of many of these galaxies appear elsewhere at higher resolution (e.g., Sandage 1961). The Schmidt *B* photographs are included in this atlas in order to compare the *B* and *I* images from the same telescope. Gross differences between the structures seen in the two passbands then may be interpreted as a wavelength-dependent effect rather than a manifestation of different plate scales and resolutions. The granularity of the IV-N emulsions is a factor of 2 smaller than the 103a-0 emulsions, so finer detail is discernible on the *I* plates. While a blue filter used with IIIa-J (or even IV-N) plates would have provided a better comparison of the features in the *B* and *I* passbands, the increase by a factor of 2 in total telescope time needed would have been unwarranted for the comparatively small benefits.

Most of the *I* plates were exposed with considerable moonlight present; typically the galaxies were observed when they were more than 30° away from the moon at its 0.5 to 1.0 phase. The *B* plates were exposed with a dark or nearly dark sky. The sky densities of the plates are, on the average, 0.7 to 1.5 above plate fog on the *I* plates, and 0.3 to 0.6 above plate fog on the *B* plates. The sky backgrounds of the *B* and *I* plates have been matched in the reproductions in Figures 1 through 19 in order to simplify comparisons.

Calibration wedges were placed on an unexposed end of each plate with a Gunn sensitometer using the appropriate filter immediately after each galaxy exposure. The exposure times for the wedges were within 30% of the galaxy exposure times. The characteristic curves of several representative plates were measured by scanning the calibration wedges with a densitometer. The slope, γ, on a density versus log (intensity) plot was determined to be about 2.5 times larger for the *I* plates than for the *B* plates, so that the *I* plates have a higher contrast.

The photographs in Figures 1 through 19 were printed with polycontrast paper, and the inherent contrasts on the plates have been reproduced as accurately as possible. An inspection of the plates confirms that the photographs were not reproduced at different contrasts. Because of the more limited dynamical range of emulsions on paper compared with plates, the faintest and brightest features cannot be reproduced in a single photograph. The central regions of many or most of the photographs are saturated, since it was more desirable to show the fainter features than the brighter ones. The original plates reveal more details about the innermost

regions, which do not affect the conclusions about the blue and near-infrared structure described in this paper.

c) *Preliminary Intensity Estimates*

Quantitative analyses of the galaxies in this atlas will be made when all of the plates have been scanned with a microdensitometer. However, in order to provide a guideline for examining and comparing the galaxy photographs, some initial results will be described. These are not intended to be exact, but are merely illustrative.

Photoelectric photometry data in the *B* and *I* passbands previously were obtained for six of the galaxies in this atlas: NGC 3031, 4321, 5194, 5457 (Schweizer 1976), and NGC 628 and 7793 (Elmegreen 1980*a*). Apertures of 17.″8 and 16.″0, respectively, were used. Each galaxy was measured at 6 to 11 points on its E-W axis. A point-by-point comparison of these results indicates that the surface brightnesses typically are 2 mag arcsec^{-2} fainter in the *B* than in the *I*. The central regions average 19.3 ± 1.0 mag arcsec^{-2} in the *B* and 17.3 ± 1.3 mag arcsec^{-2} in the *I*, while the outer regions are 23 to 24 mag arcsec^{-2} in the *B* and 21 to 22 mag arcsec^{-2} in the *I*.

Several galaxies (NGC 2403, 4321, 5033, 5248) were examined in order to estimate the relative intensities of the features seen in the galaxy photographs. Arm and interarm densities were visually determined with a step wedge, and intensities were obtained from the characteristic curves. In all cases, the figures quoted below should be regarded as upper limits since the largest errors result for features that are close to the sky brightness. In NGC 2403, the arms are brighter than the interarm regions by about 130% in the *B*, and 40% in the *I*. In NGC 4321, the average arm intensity, excluding the brightest areas, is 170% brighter than the interarm for both the *B* and the *I* plates. In NGC 5033, the arms are about 270% brighter than the interarm in the *B*, and 130% brighter in the *I*. In NGC 5248, the arms are brighter than the interarm by a factor of 2 in the *B*, and an upper limit of 18 in the *I*.

Selected surface photometry of the galaxies NGC 628, 5194, 5457, and 7793 (Elmegreen 1980*a*) provides more details regarding the intensities of different features. A total of 44 dusty regions were measured relative to their surrounding neighborhood; these features are identified in the above paper. In the *B* band, these dust areas are 0.3 to 1.4 mag fainter than nearby comparison regions; in the *I*, the differential magnitudes range from 0.1 to 0.6.

It is instructive to consider the differential magnitudes that correspond to different intensity enhancements. A spiral arm with a 5% amplitude relative to its surroundings is only 0.05 mag brighter than the interarm. Such a pattern would be difficult to measure even with surface photometry. A 10% amplitude would result in an 0.1 mag differential, which can be measured. The arms in NGC 4321 are ~1.1 mag brighter than the interarm regions. Features with a 20% enhancement would be easy to recognize on the photographs (e.g., the dust regions mentioned previously); most of the arms in both the *B* and *I* passbands are probably considerably brighter than this, based on the previous estimates. The detection of fainter patterns will require microdensitometer measurements. Therefore, the simplistic divisions into grand design and flocculent galaxies in this atlas represent gross separations based on the presence or absence of smooth continuous arms showing a conservatively estimated 20% or more enhancement over the interarm regions.

III. DISCUSSION

Smooth red arms in M51 were discovered by Zwicky (1955) through the superposition of two plates exposed in different passbands. Their existence was confirmed by the multicolor surface photometry and image-tube photograph made by Schweizer (1976). Jensen (1977) and Elmegreen (1979) subsequently found spiral structure in the near-infrared passband for other galaxies.

One dominant feature in the grand design spiral galaxies is emphasized by the near-infrared photographs in this atlas and in previous papers. This characteristic is the highly symmetric two-armed spiral pattern. The two main spiral arms show a remarkable degree of smoothness and continuity, particularly in the central regions of grand design spirals. In the barred spiral galaxies, this bimodal pattern manifests itself throughout most of the visible structure.

Many of the galaxies have multiple spiral arms and branches; these are common in later type spirals (Sandage 1961). Multiple arms or branches are part of the regular spiral pattern, and all have the same pitch angle. The arms can be traced back to the central regions. These multiple arms appear in the *I* as well as in the *B* photographs. The multiple arms are smoother in the near-infrared, as are the two main spiral arms.

In addition to multiple arms, in many galaxies there are spurs that jut out from the main spiral arms (Weaver 1970, Elmegreen 1980*b*). The spurs are distinct from branches in that they have a greater pitch angle, and are short segments that do not participate in the basic spiral pattern. The spurs are prominent in both the *B* and *I* passbands also.

The primary characteristic of flocculent spiral galaxies is the disjoint nature of the individual arms. The prototype is NGC 2841, but many galaxies in this category differ considerably from this galaxy in their appearance. The number or openness of the arms is not a factor in determining whether a galaxy is flocculent. For example, NGC 7793 is a flocculent spiral galaxy because its spiral arms are fragmented and patchy. The spiral pattern of NGC 2841 clearly is more regular than that of NGC 7793, but this difference is primarily a

function of Hubble type. NGC 2841 is an earlier type galaxy than NGC 7793, so it has a more orderly overall design.

Flocculent spiral galaxies do not appear smoother in the near-infrared on the photographs in this atlas; their arms are as patchy in the *I* as they are in the *B*. This is in contrast with the grand design spiral galaxies. The patchiness of the flocculents probably reflects the presence of H II regions and complexes of OB and supergiant associations. In this atlas, no underlying bimodal symmetry with an amplitude of some 20% or more can be discerned in the flocculent galaxies, although such bright two-armed patterns clearly are present in the near-infrared for all galaxies classified as grand design spirals. Thus, the morphology of flocculent spiral galaxies is qualitatively distinct from that of grand design galaxies. Forthcoming quantitative results will form the basis for more definitive categorization.

I am grateful to Dr. Bruce Elmegreen for suggesting this survey, and acknowledge helpful discussions with him and Drs. Alan Dressler and Kevin Prendergast. I thank an anonymous referee for his suggestions and comments on the manuscript, John Bedke and Douglas Cunningham for reproducing the galaxy figures, and the staff of the Mt. Wilson and Las Campanas Observatories and Palomar Observatory for the generous allotment of telescope time which made this survey possible. A Carnegie postdoctoral fellowship from the Carnegie Institution of Washington is gratefully acknowledged.

REFERENCES

de Vaucouleurs, G., de Vaucouleurs, A., and Corwin, H. G., Jr. 1976, *Second Reference Catalogue of Bright Galaxies* (Austin: University of Texas Press).
Elmegreen, B. G. 1979, *Ap. J.*, **231**, 372.
Elmegreen, D. M. 1979, Ph.D. thesis, Harvard University.
_____. 1980*a*, *Ap. J. Suppl.*, **43**, 37.
_____. 1980*b*, *Ap. J.*, **242**, 528.
Gerola, H., and Seiden, P. E. 1978, *Ap. J.*, **223**, 129.
Hoessel, J. G. 1978, *AAS Photo-Bulletin*, **17**, 10.
Jenkins, R. L., and Farnell, G. C. 1976, *J. Photographic Sci.*, **24**, 41.
Jensen, E. B. 1977, Ph.D. thesis, University of Arizona.
Jensen, E. B., Talbot, R. J., and Dufour, R. J. 1981, *Ap. J.*, **243**, 716.
Johnson, H. L. 1966, *Stars and Stellar Systems*, Vol. **7**, *Nebulae and Interstellar Matter*, ed. B. M. Middlehurst and L. H. Aller (Chicago: University of Chicago Press), p. 167.
Kormendy, J. 1977, *The Evolution of Galaxies and Stellar Populations*, ed. B. M. Tinsley and R. B. Larson (New Haven: Yale University Printing Service), p. 131.
Lin, C. C., and Shu, F. H. 1964, *Ap. J.*, **140**, 646.
Mueller, M. W., and Arnett, W. D. 1976, *Ap. J.*, **210**, 670.
Pinto, L. 1979, *AAS Photo-Bulletin*, **21**, 6.
Roberts, W. W., Roberts, M. S., and Shu, F. H. 1975, *Ap. J.*, **196**, 381.
Sandage, A. 1961, *The Hubble Atlas of Galaxies* (Washington: The Carnegie Institution of Washington).
_____. 1975, *Stars and Stellar Systems*, Vol. **9**, *Galaxies and the Universe*, ed. A. Sandage, M. Sandage, and J. Kristian (Chicago: University of Chicago Press), p. 1.
Schweizer, F. 1976, *Ap. J. Suppl.*, **31**, 313.
Schoening, W. E. 1978, *AAS Photo-Bulletin*, **17**, 12.
Weaver, H. 1970, *IAU Symposium 39, Interstellar Gas Dynamics*, ed. H. Habing (Dordrecht: Reidel), p. 22.
Woltjer, L. 1965, *Stars and Stellar Systems*, Vol. **5**, *Galactic Structure*, ed. A. Blaauw and M. Schmidt (Chicago: University of Chicago Press), p. 531.
Zwicky, F. 1955, *Pub. A.S.P.*, **67**, 232.

D. M. ELMEGREEN: The Mount Wilson and Las Campanas Observatories, 813 Santa Barbara Street, Pasadena, CA 91101

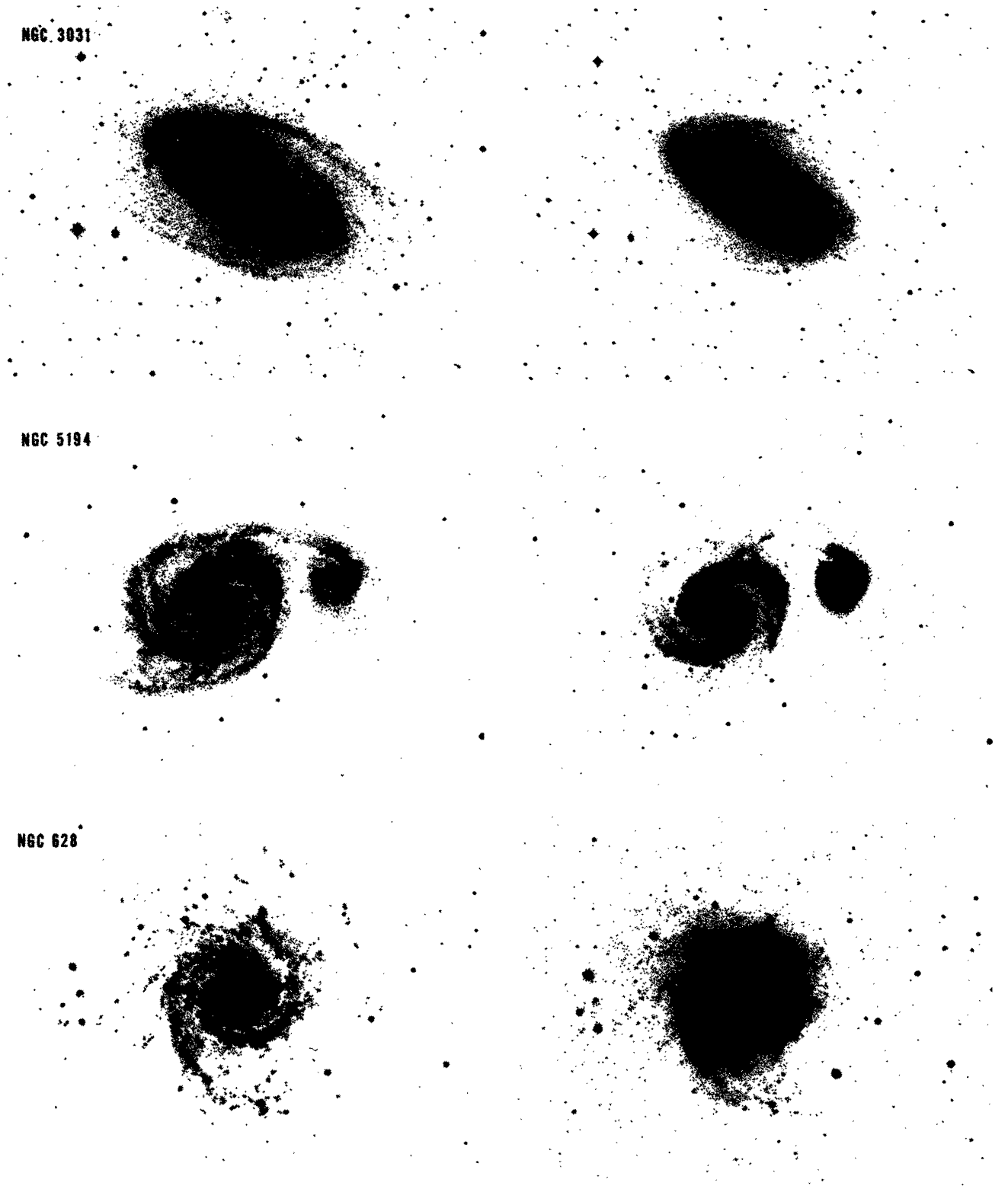

FIG. 1.—All of the following figures show the blue (103a-0+GG13) photographs on the left, and the near-infrared (IV-N+Wr 88A) on the right. NGC 3031: north is to the right. NGC 5194: N is to the right. NGC 628: N is to the top.

ELMEGREEN (*see* page 230)

PLATE 2

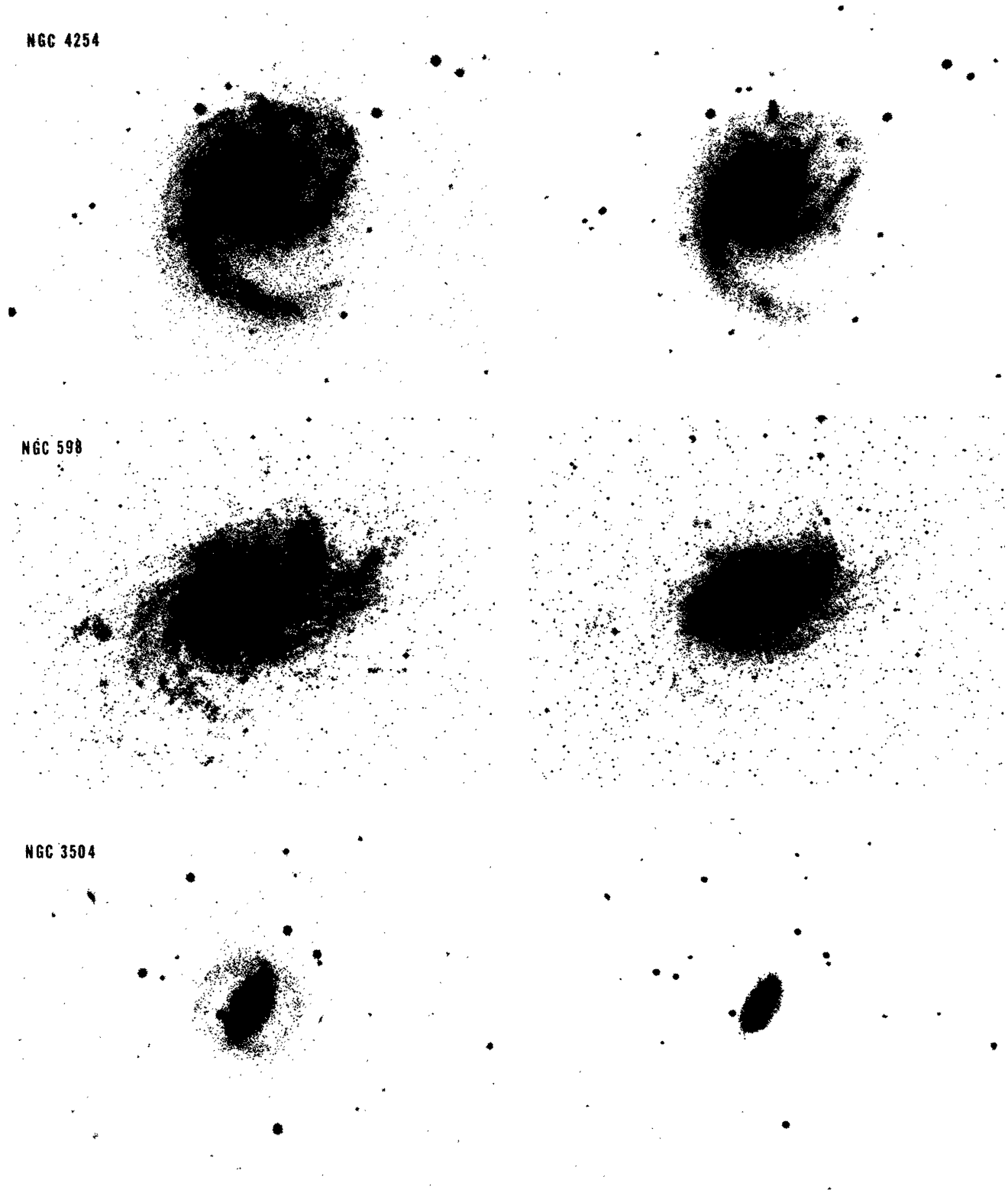

FIG. 2.—NGC 4254: N is to the right. NGC 598: N is to the right. NGC 3504: N is to the top.

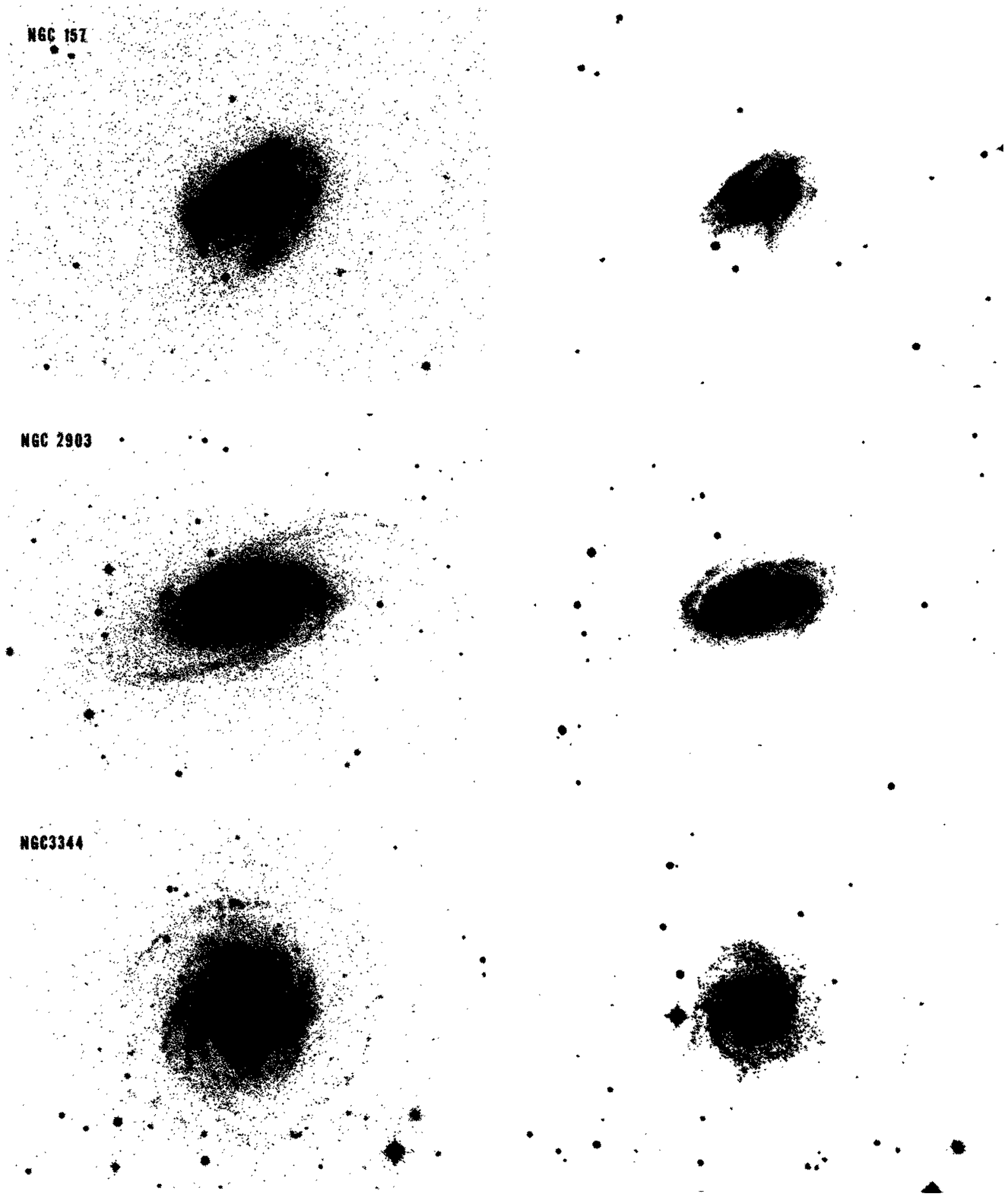

FIG. 3.—NGC 157: N is to the right. NGC 2903: N is to the right. NGC 3344: N is to the top.

ELMEGREEN (*see* page 230)

PLATE 4

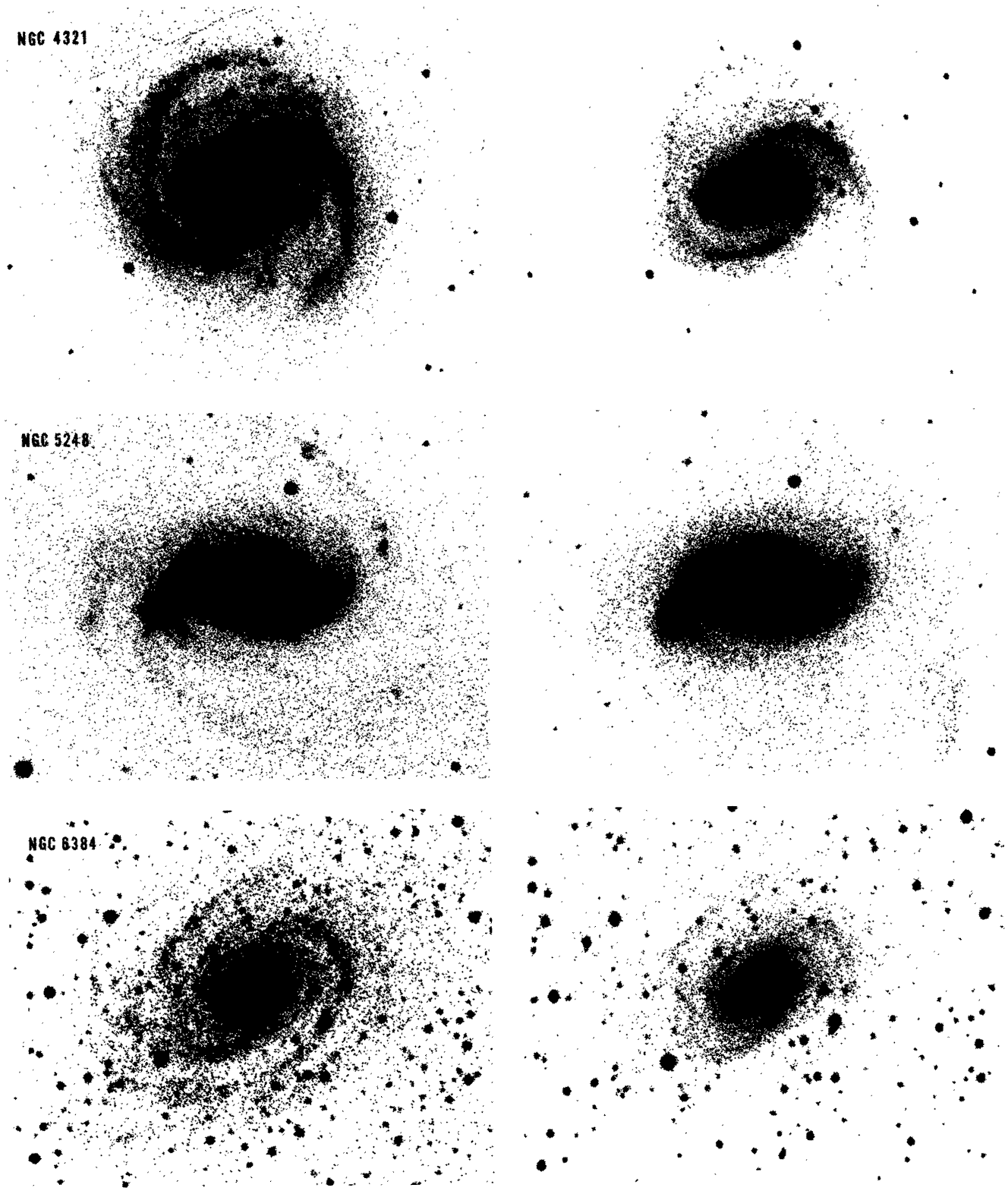

FIG. 4.—NGC 4321: N is to the top. NGC 5248: N is to the lower left corner. NGC 6384: N is to the right.

ELMEGREEN (*see* page 230)

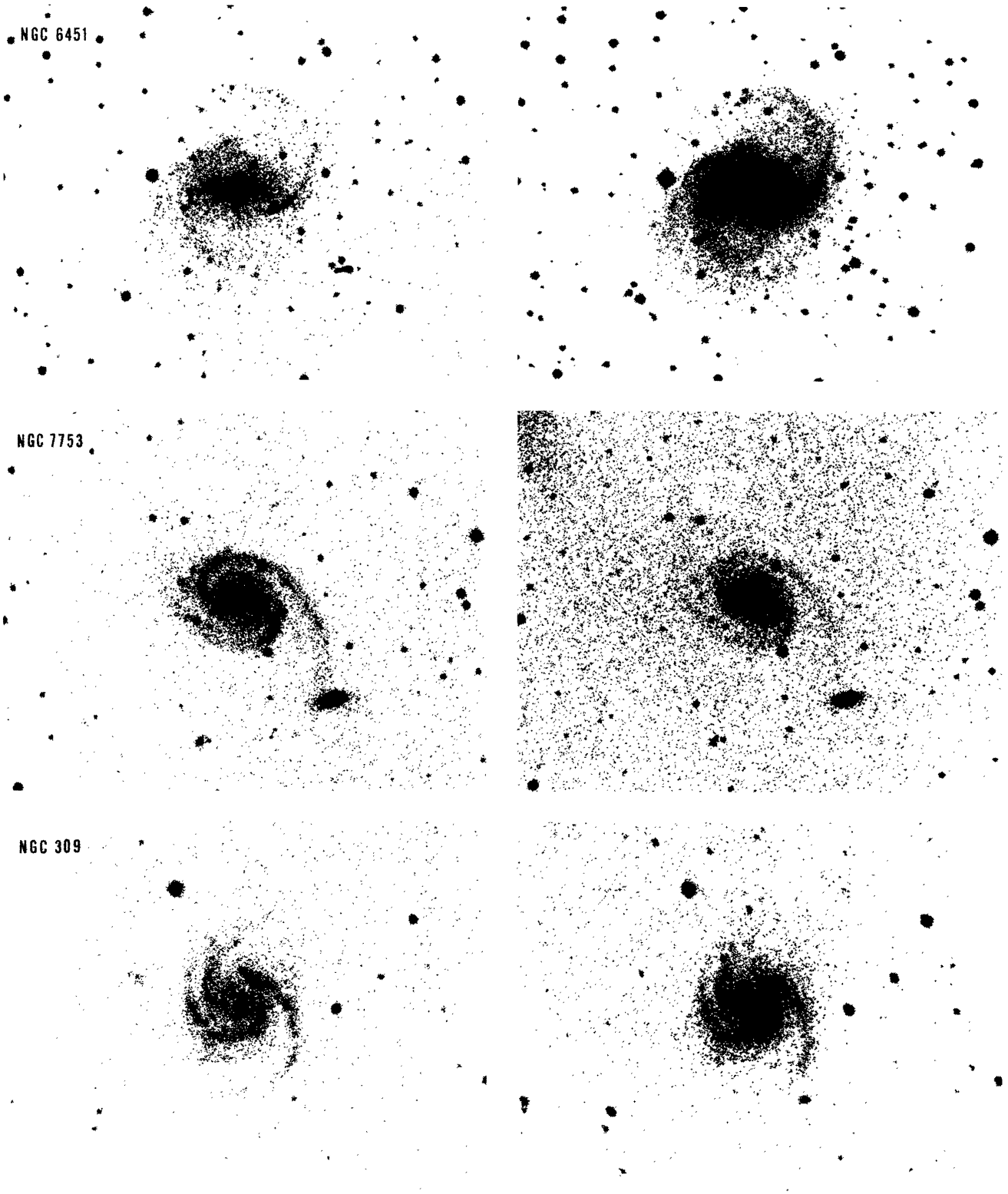

FIG. 5.—N is to the top in all photographs. NGC 6951 is mislabeled as NGC 6451 in upper photograph.

ELMEGREEN (*see* page 230)

PLATE 6

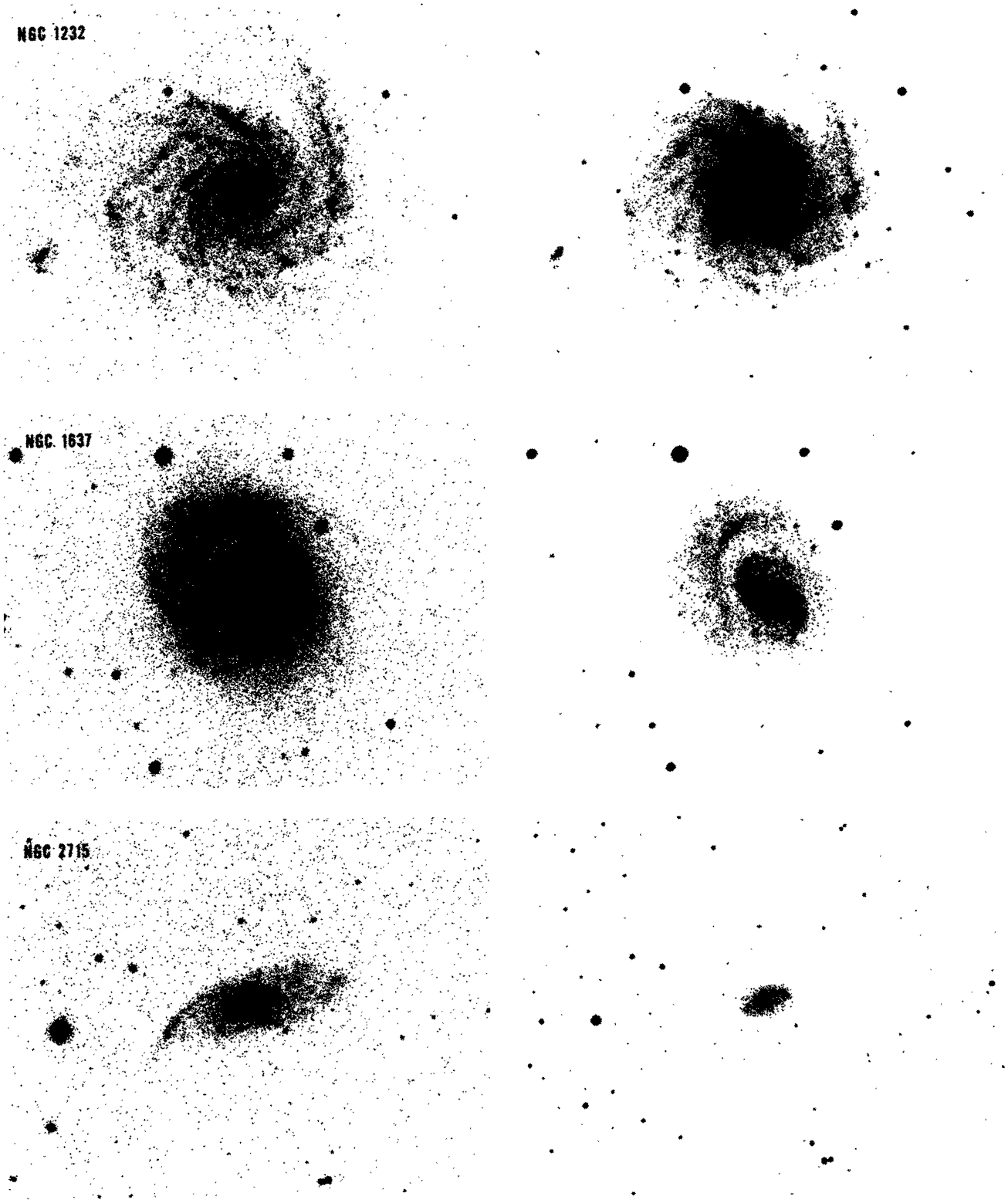

FIG. 6.—NGC 1232: N is to the top. NGC 1637: N is to the top. NGC 2715: N is to the right.

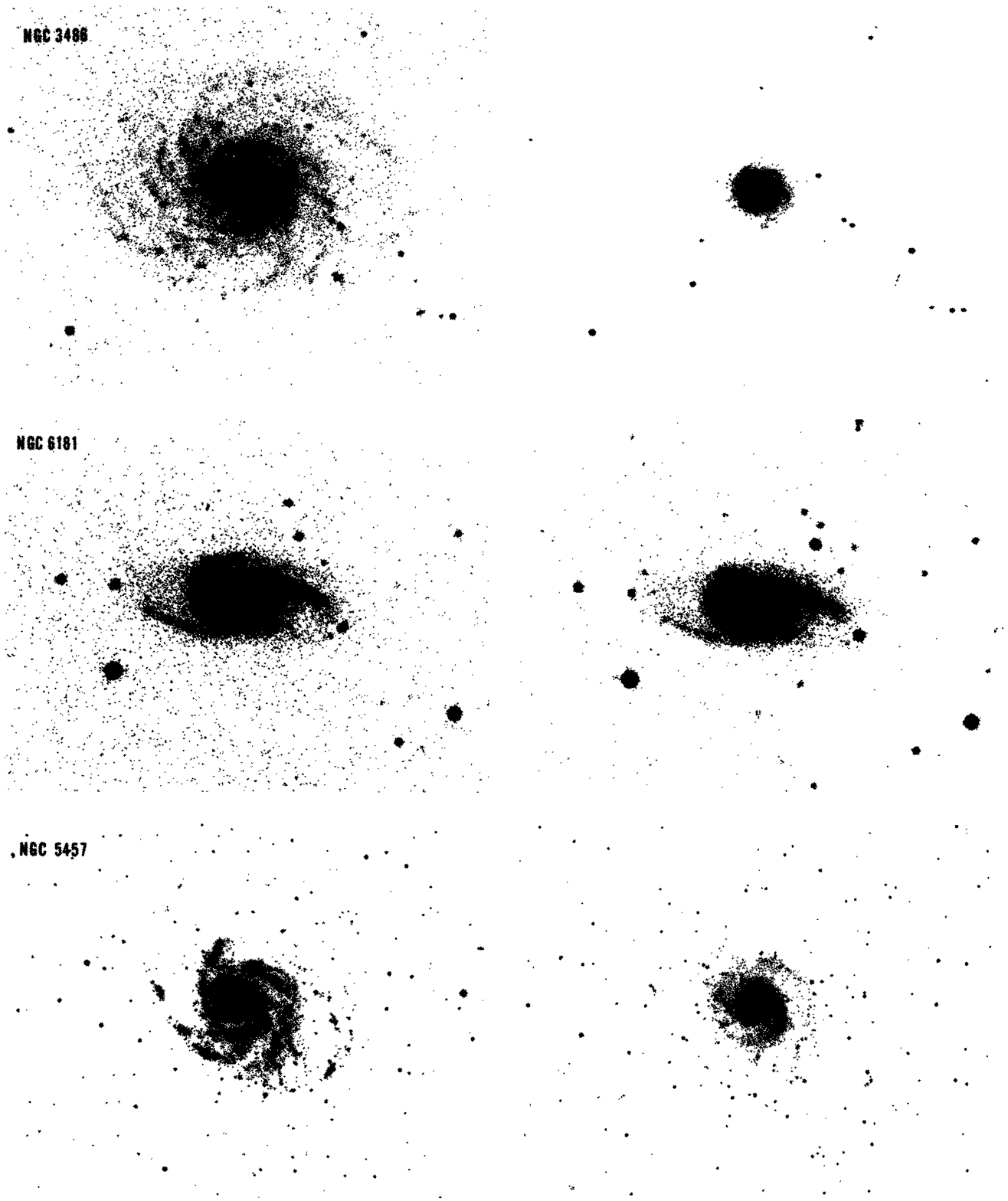

FIG. 7.—NGC 3486: N is to the top. NGC 6181: N is to the right. NGC 5457: N is to the top.

ELMEGREEN (*see* page 230)

PLATE 8

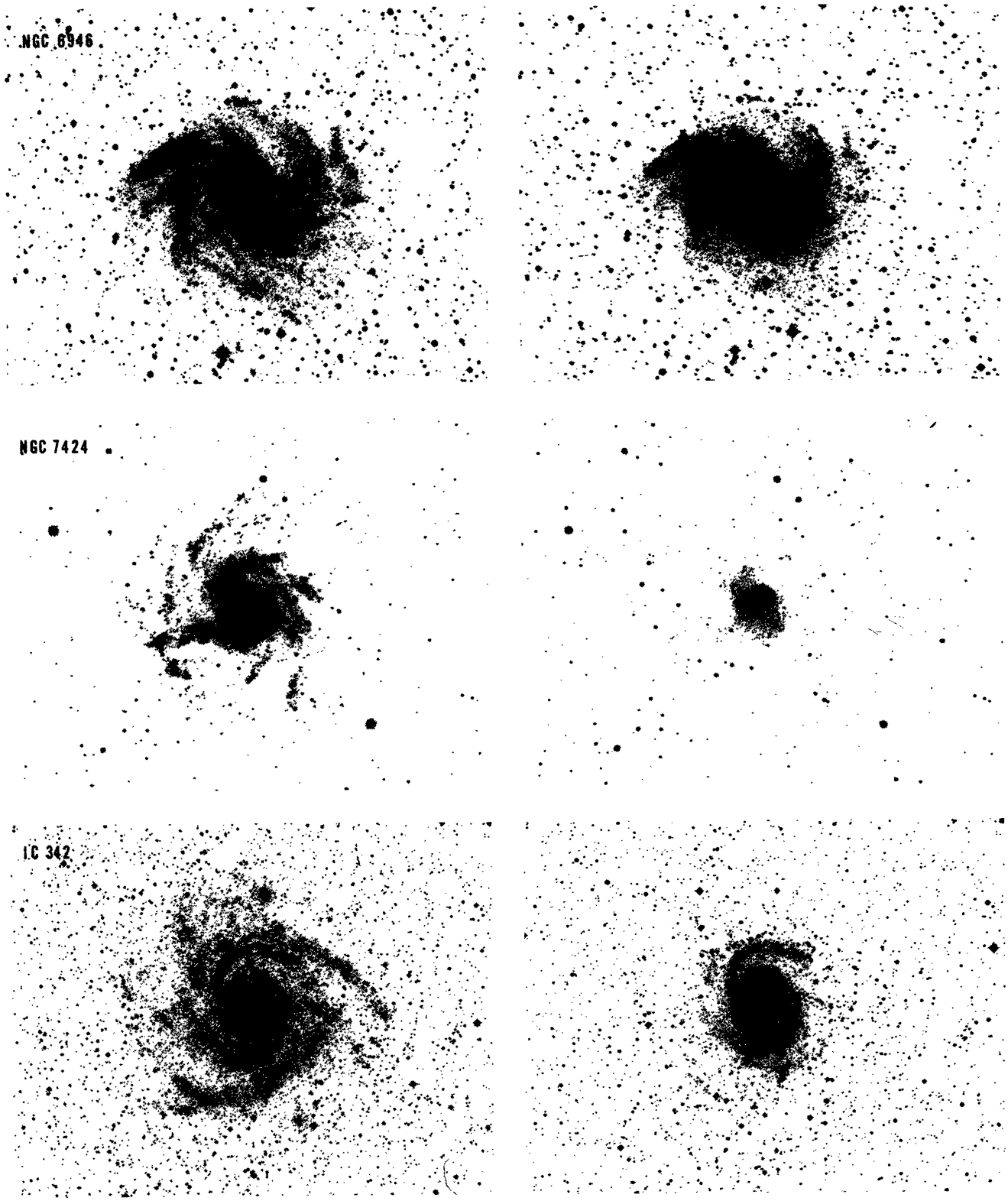

FIG. 8.—N is to the top in all photographs

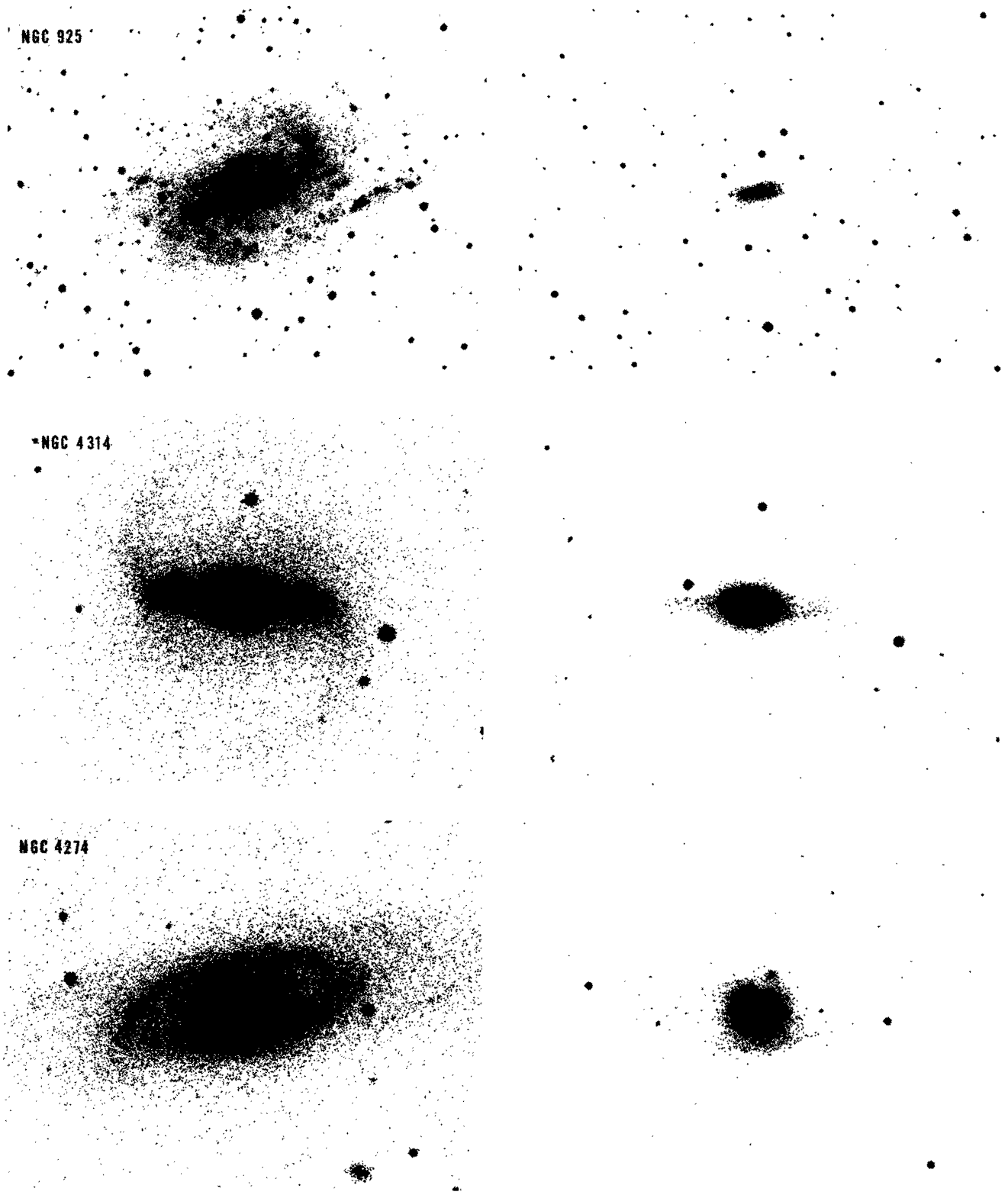

FIG. 9.—NGC 925: N is to the top. NGC 4314: N is to the lower right corner. NGC 4274: N is to the top.

PLATE 10

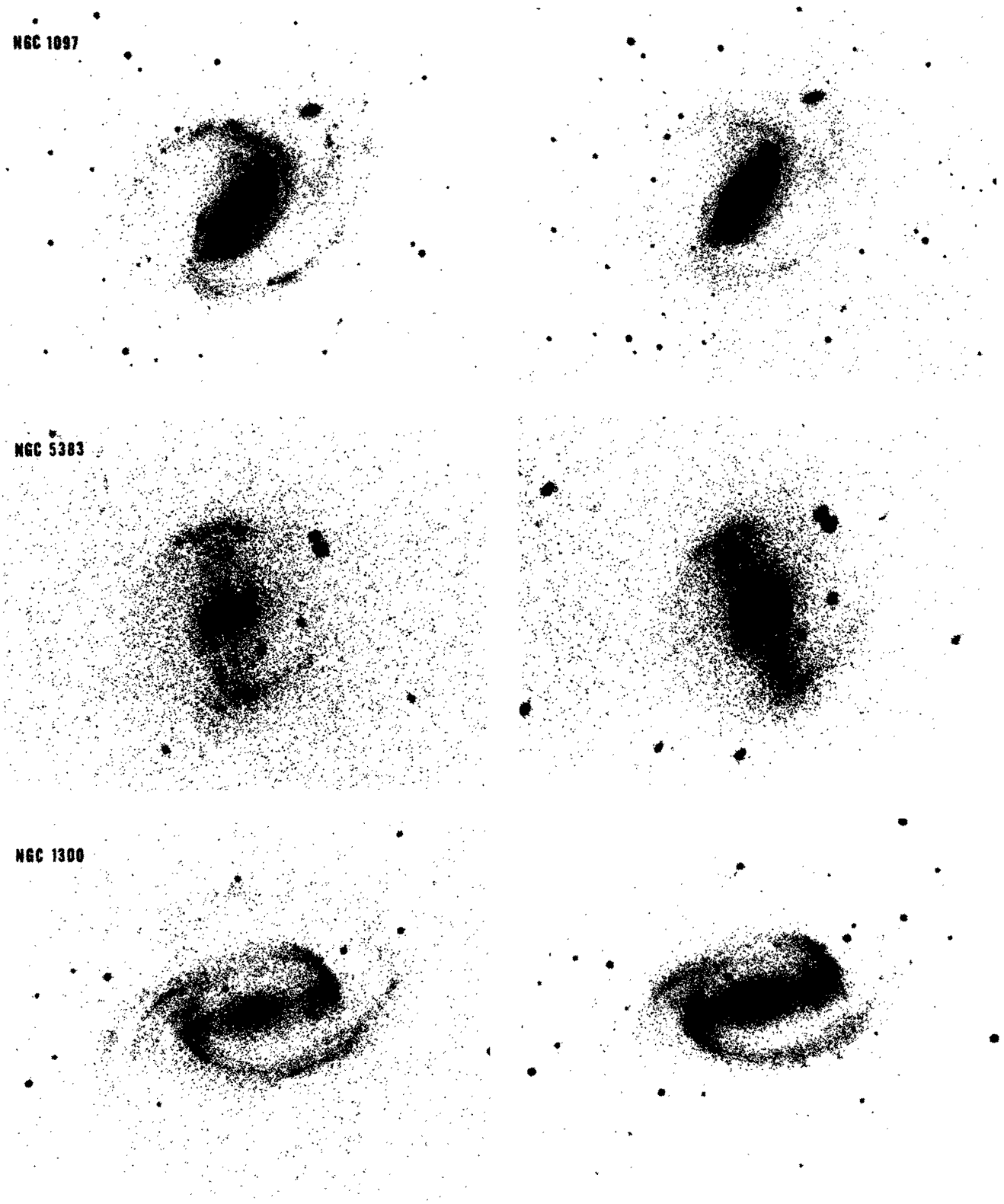

FIG. 10.—NGC 1097: N is to the top. NGC 5383: N is to the right. NGC 1300: N is to the top.

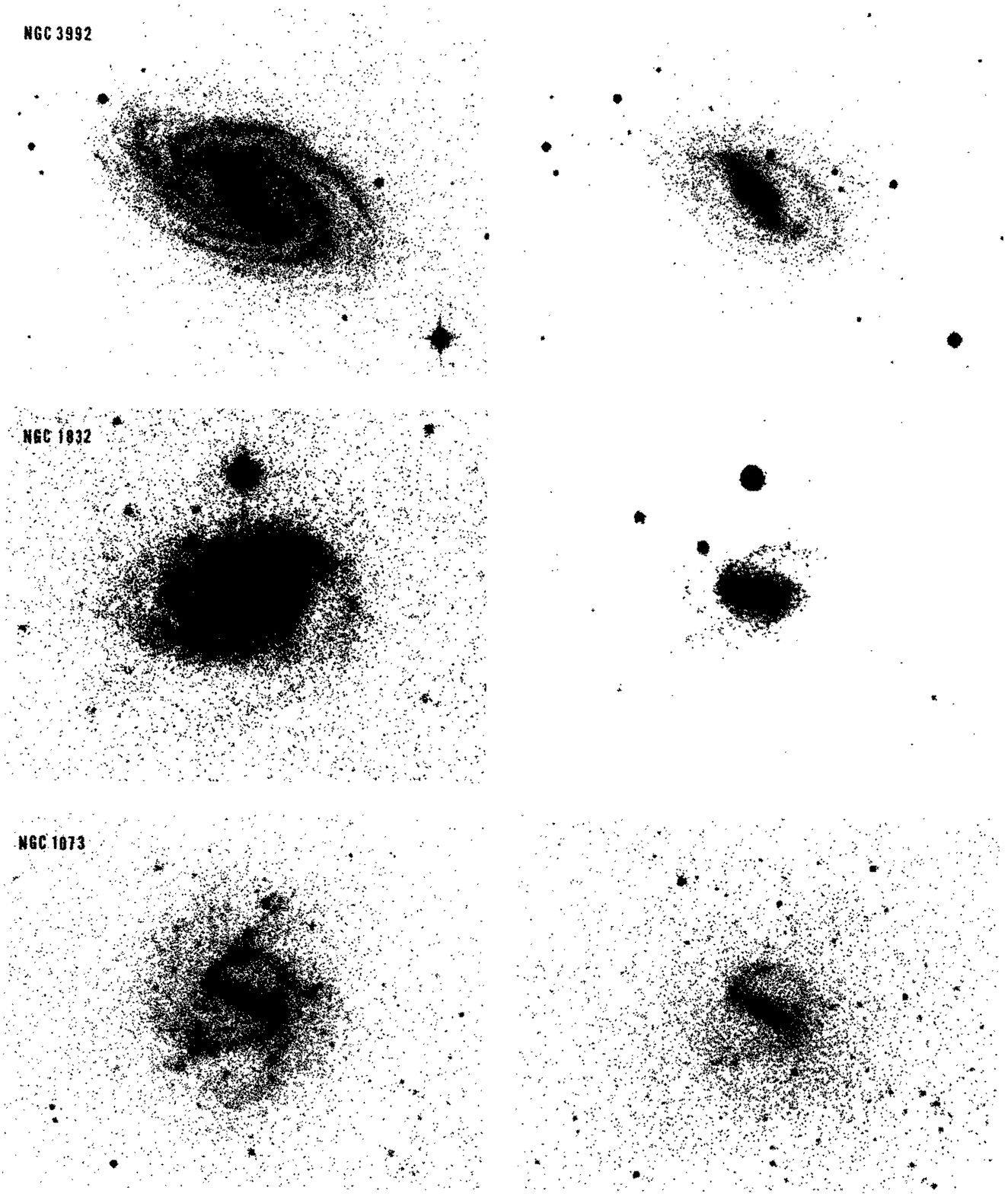

FIG. 11.—NGC 3992: N is to the top. NGC 1832: N is to the right. NGC 1973: N is to the top.

ELMEGREEN (*see* page 230)

PLATE 12

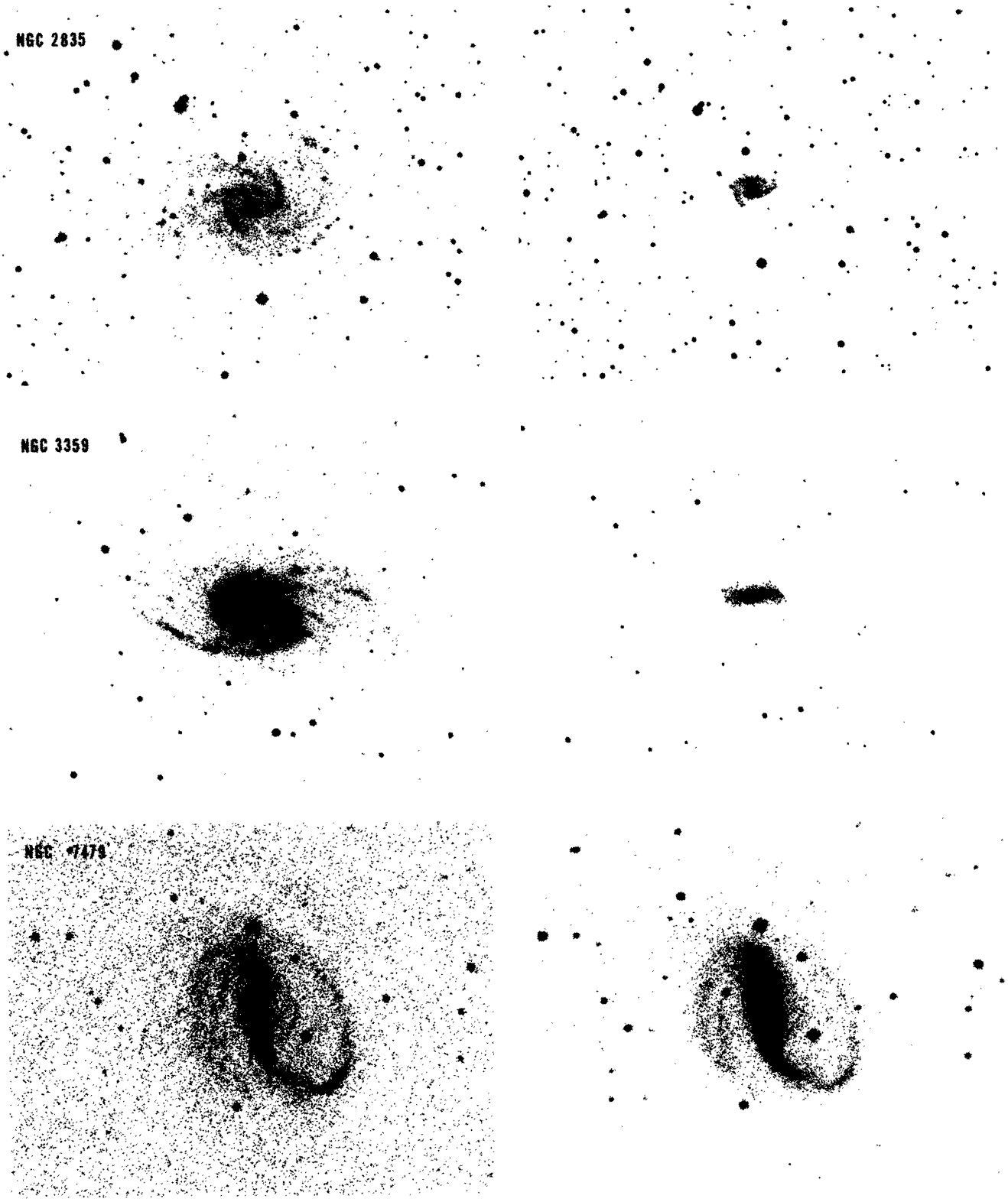

FIG. 12.—NGC 2835: N is to the right. NGC 3359: N is to the right. NGC 7479: N is to the top.

ELMEGREEN (*see* page 230)

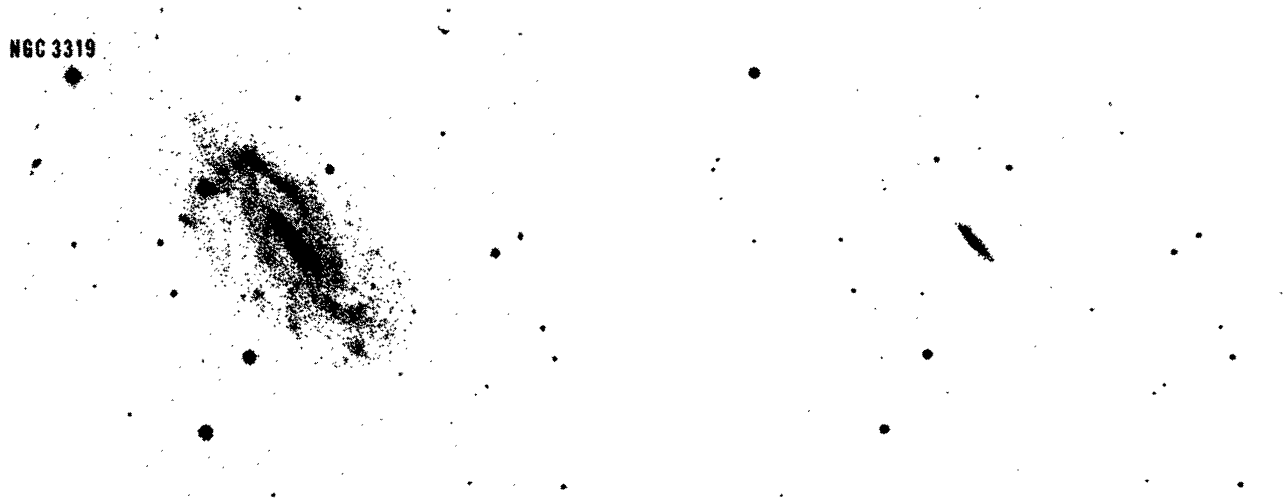

FIG. 13.—NGC 3319: N is to the top

ELMEGREEN (*see* page 230)

PLATE 14

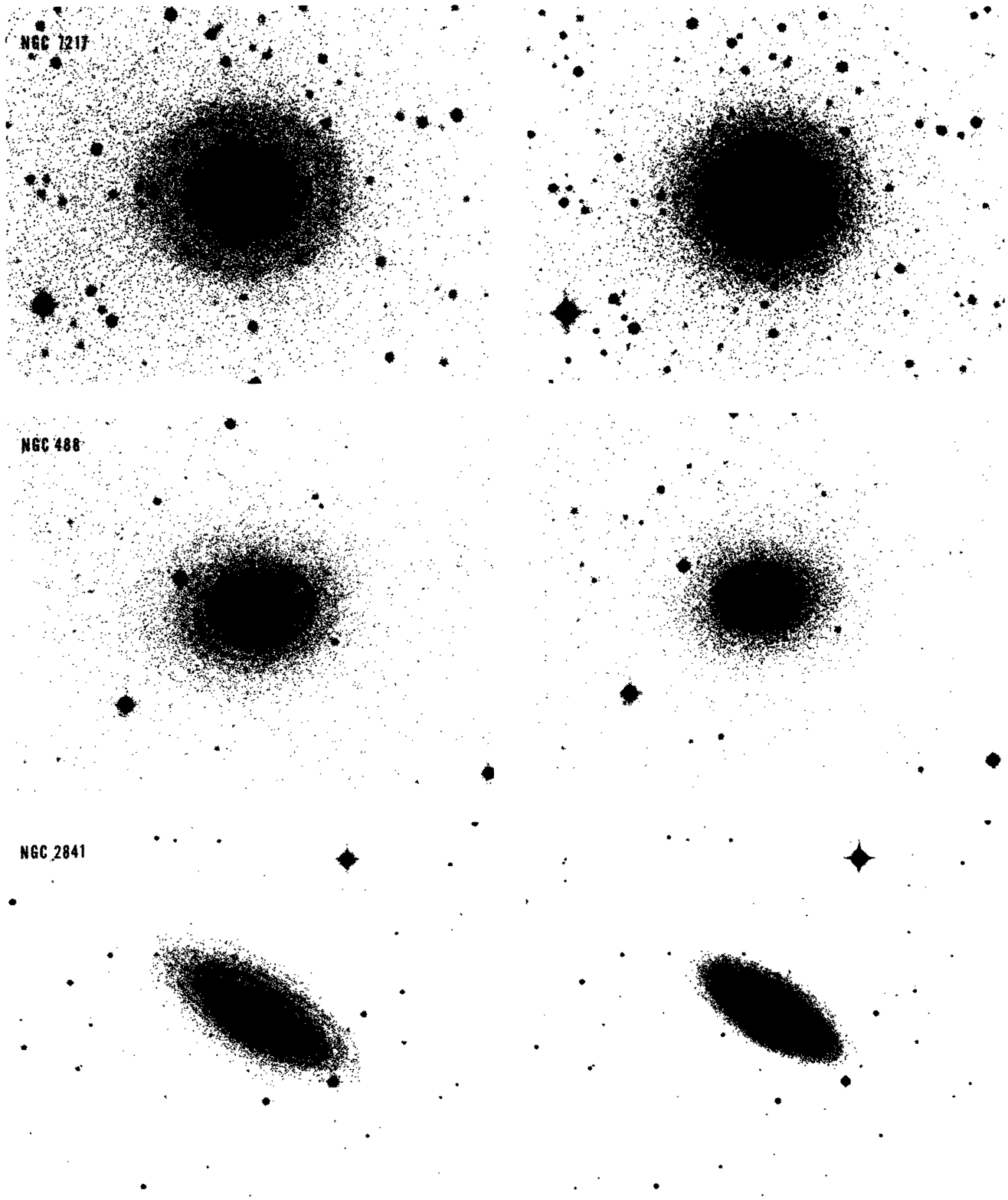

FIG. 14.—NGC 7217: N is to the top. NGC 488: N is to the right. NGC 2841: N is to the right.

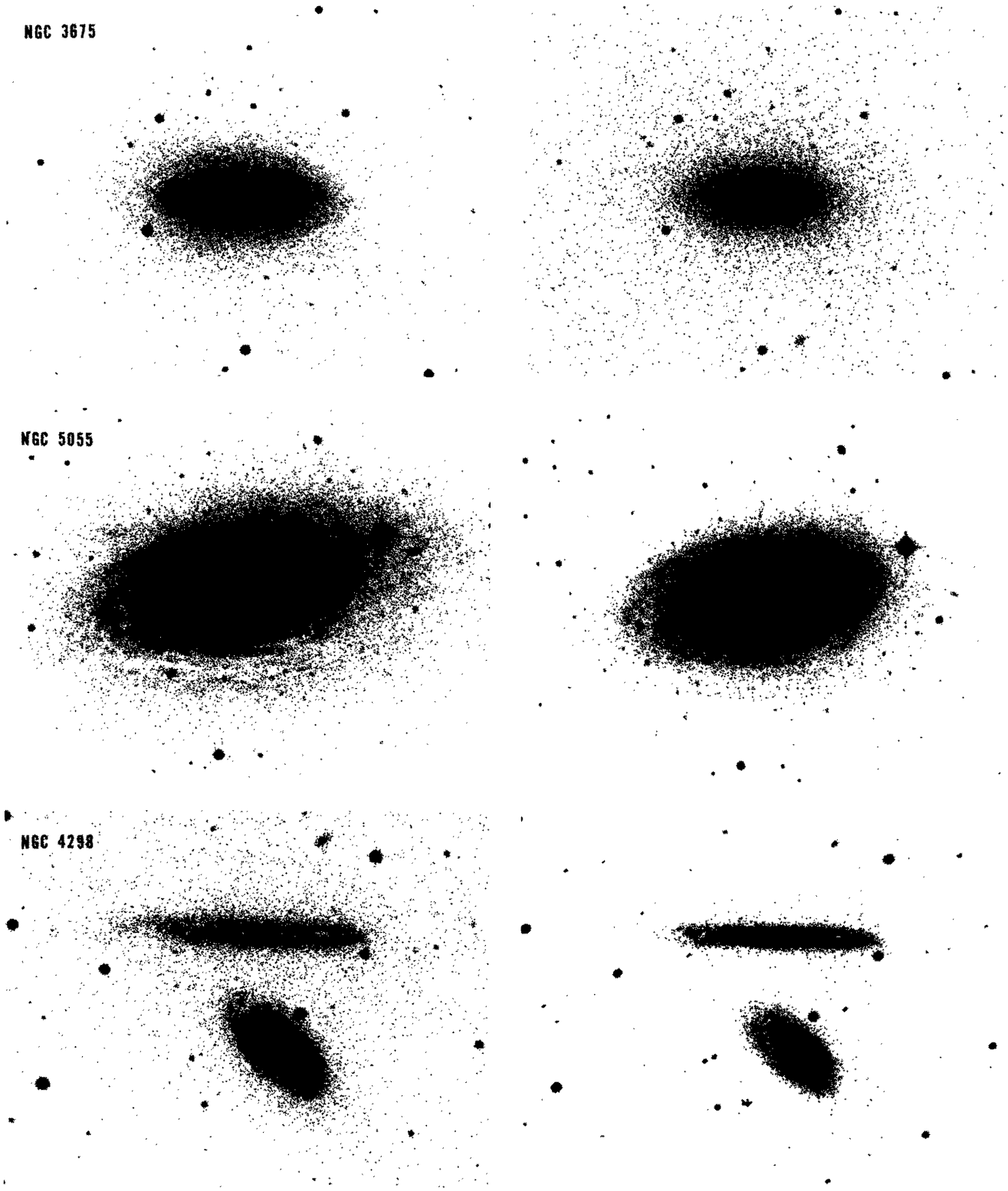

FIG. 15.—NGC 3675: N is to the right. NGC 5055: N is to the top. NGC 4298: N is to the right.

ELMEGREEN (*see* page 230)

PLATE 16

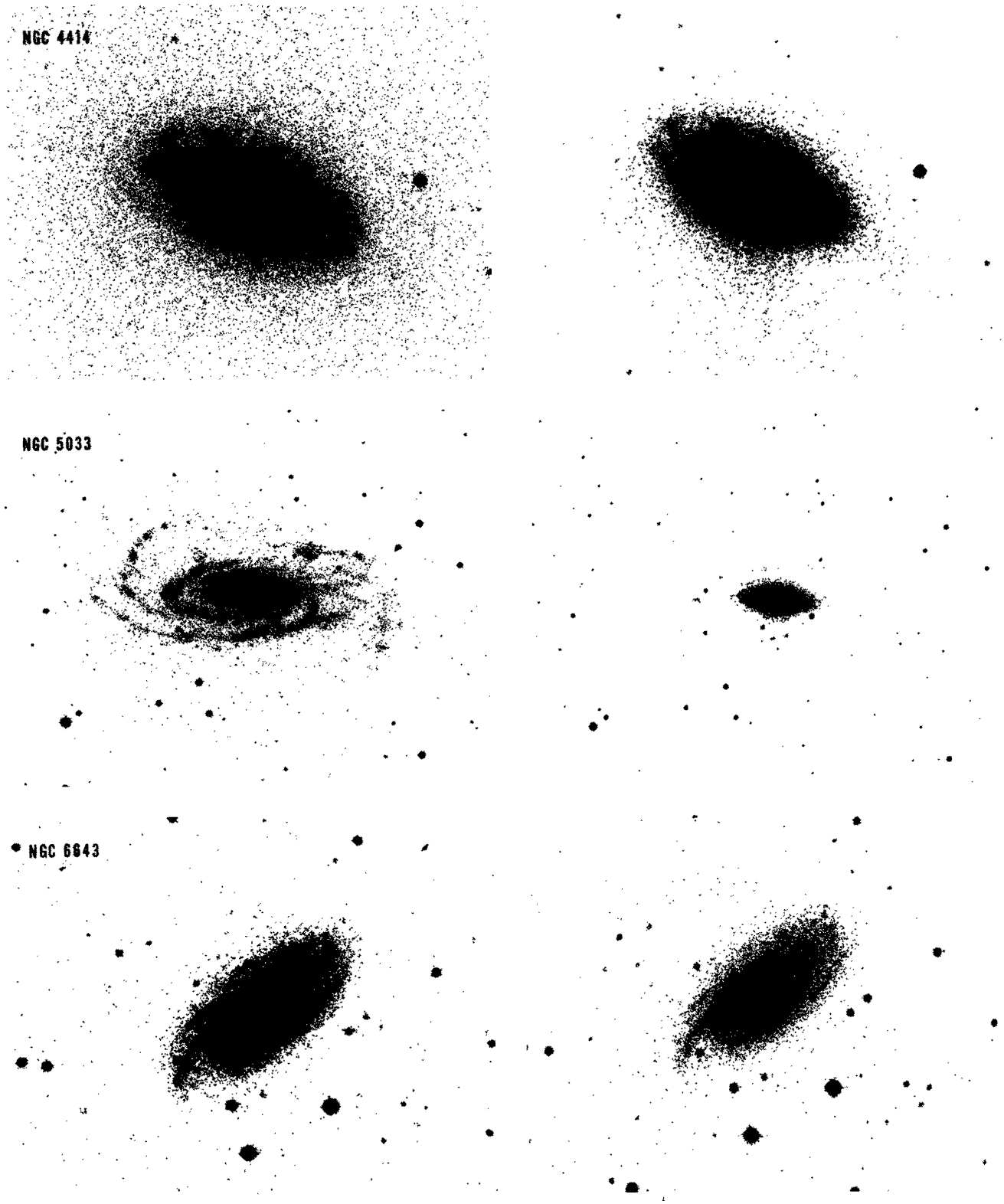

FIG. 16.—N is to the right in all photographs

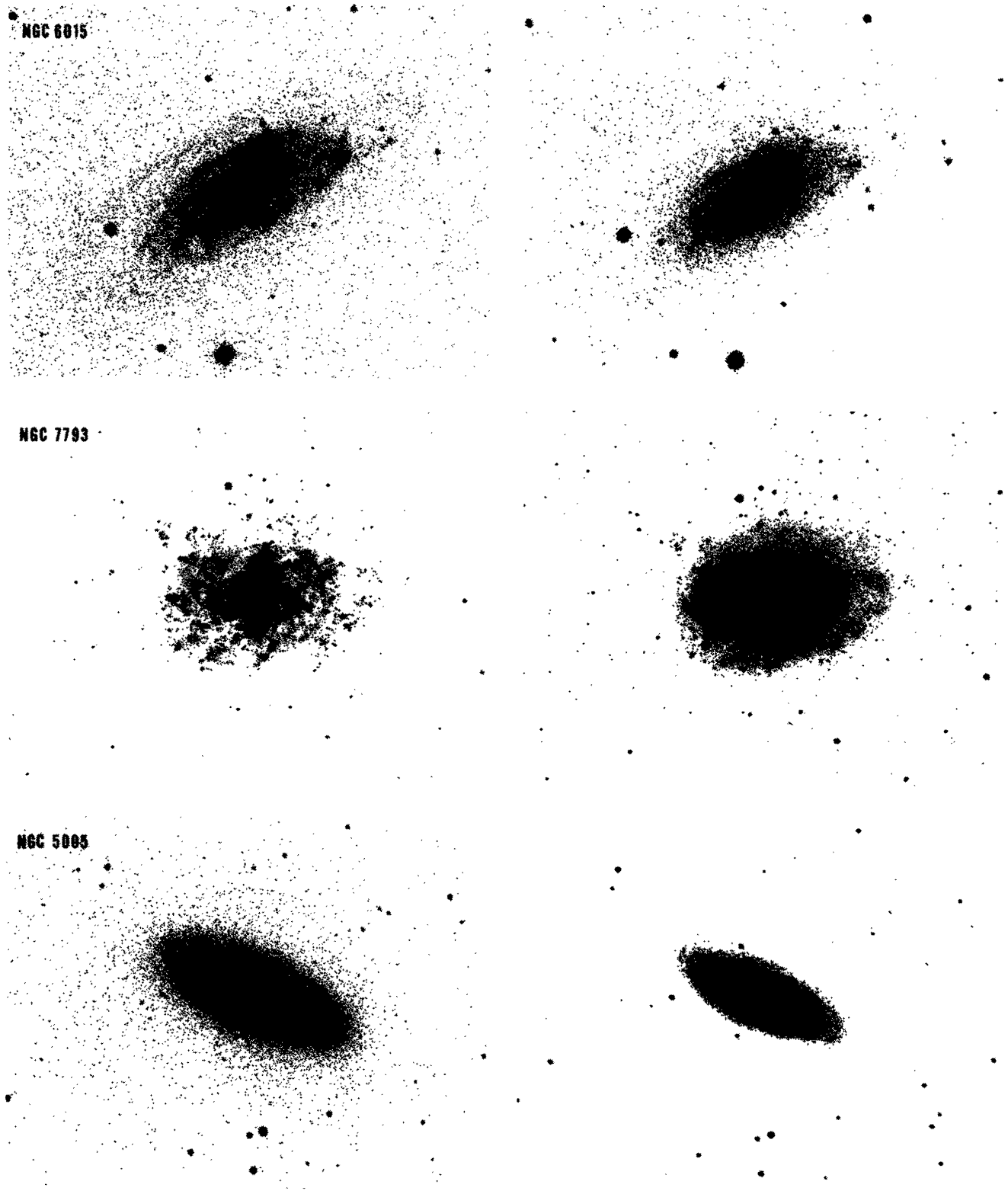

FIG. 17.—NGC 6015: N is to the right. NGC 7793: N is to the top. NGC 5005: N is to the top.

ELMEGREEN (*see* page 230)

PLATE 18

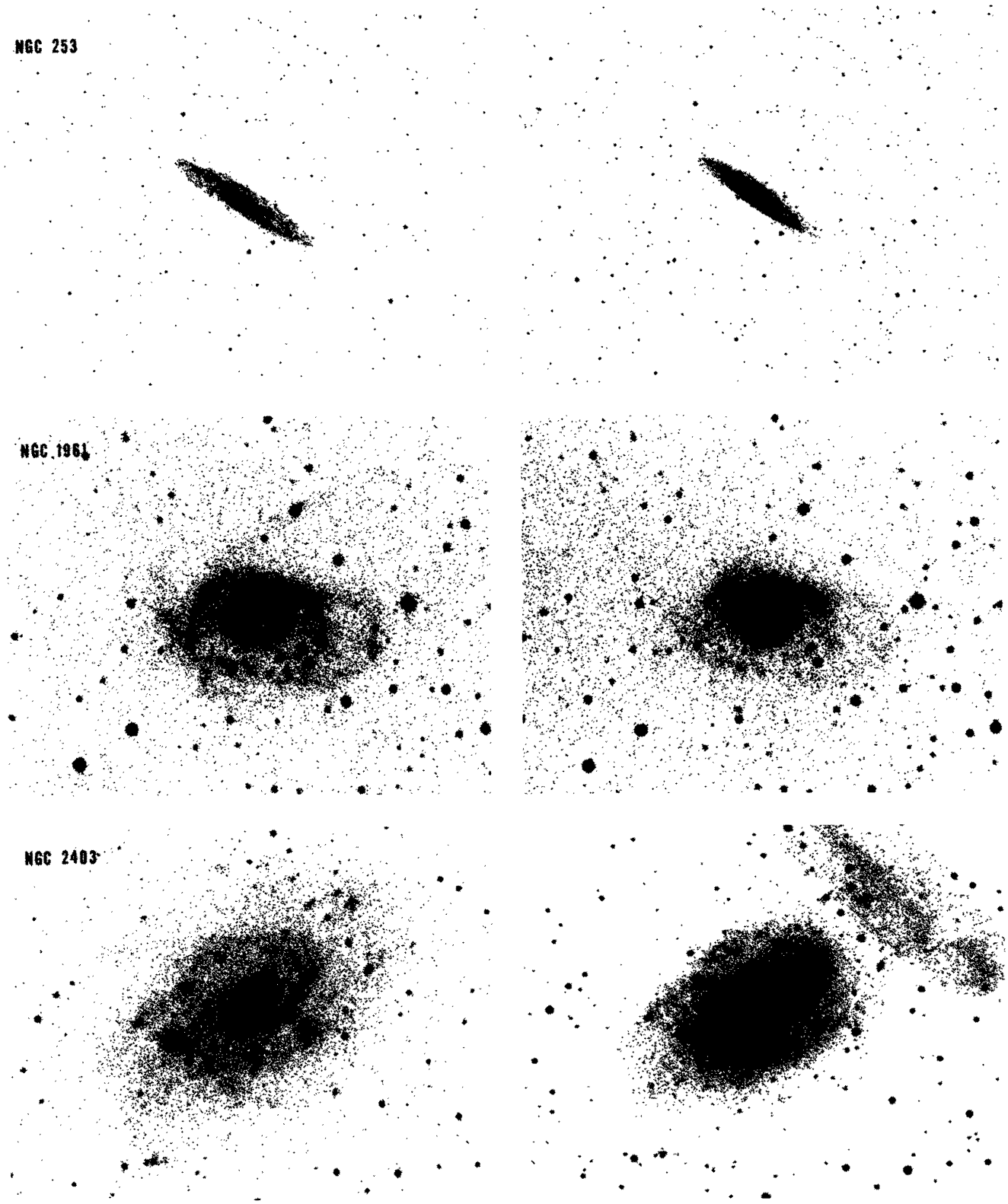

FIG. 18.—N is to the top in all photographs

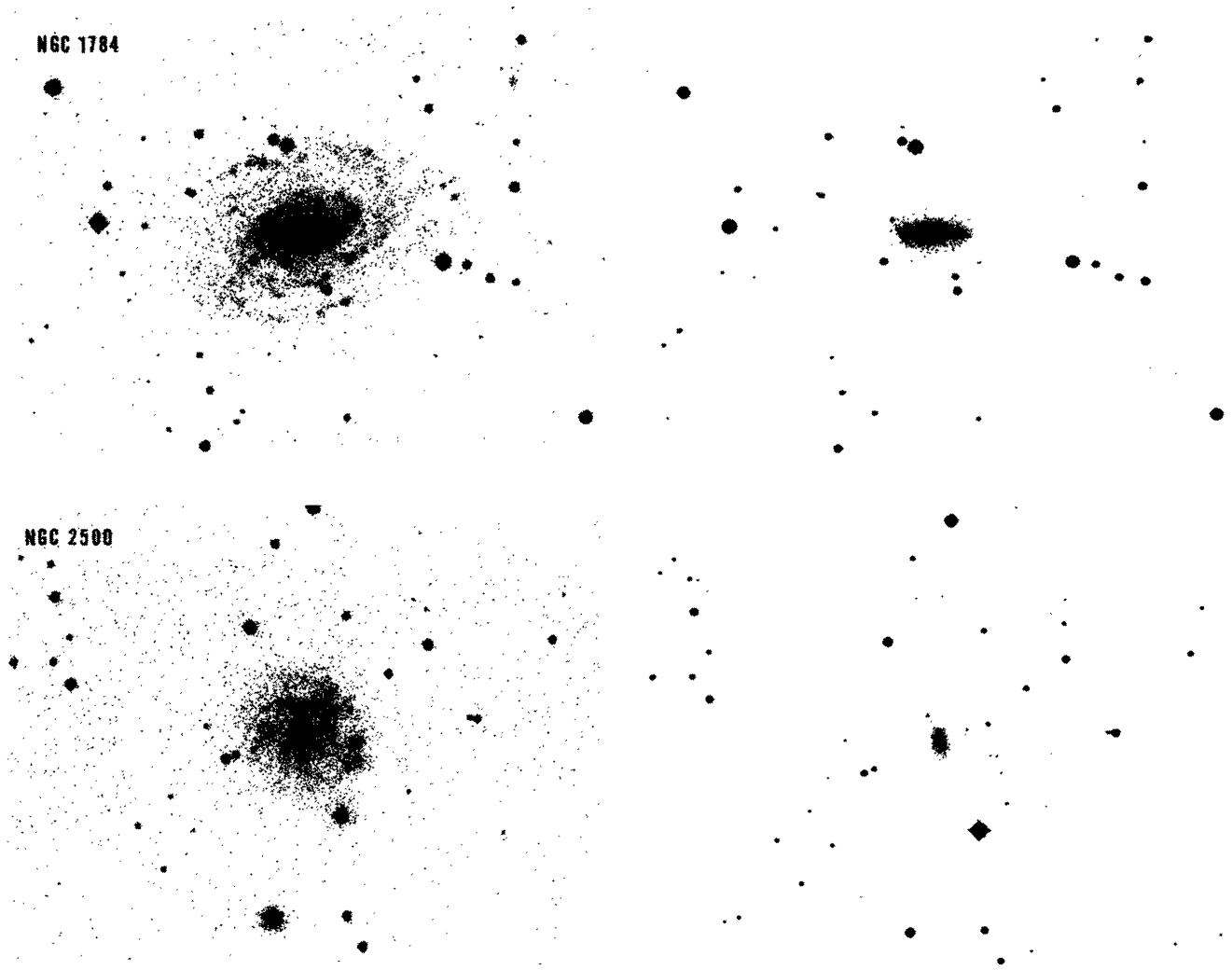

FIG. 19.—N is to the top in all photographs

ELMEGREEN (*see* page 230)